Pergamon

Journal of Structural Geology, Vol. 17, No. 6, pp. 847 to 862, 1995

0191-8141/95 $9.50 + 0.00

0191-8141(94)00109-X

Three-dimensional geometry and growth of conjugate normal faults

A. NICOL, J. J. WALSH, J. WATTERSON and P. G. BRETAN

Fault Analysis Group, Department of Earth Sciences, University of Liverpool, P.O. Box 147, Liverpool L69 3BX, U.K.

(*Received* 4 *January* 1994; *accepted in revised form* 21 *September* 1994)

Abstract—Good quality 2-D and 3-D seismic reflection data from the Timor Sea are used to determine the three-dimensional geometry, displacement patterns and development of intersecting conjugate normal faults. These data are supplemented by data from previous physical modelling studies. Conjugate structures, which comprise two intersecting opposed-dipping normal faults or fault sets, form synchronously on a geological time scale and develop due to the incidental intersection of the faults. Factors which affect both the formation and imaging of these structures include: the fault density, the spatial distribution of opposed-dipping faults, the seismic resolution and the vertical extent of the imaged fault data. Large conjugate structures grow from smaller ones; larger conjugates are associated with more numerous and larger faults than small structures. On the scale of the seismic data (fault throws range from ca 10–400 m), synchronous fault movements are accommodated by a reduction of displacements on discrete fault surfaces towards the fault intersection zone, and a corresponding increase in ductile strain of this region. High strains in the volume proximal to the fault intersection zone are expressed as thinning of stratigraphic units between the conjugate faults, and are believed to be accommodated by numerous small sub-seismic faults. Intersection of two opposed-dipping faults does not prevent their continued synchronous movement and does not result in mechanical locking of the system.

INTRODUCTION

Normal fault systems often show intersecting, opposed-dipping faults or fault arrays, or conjugates (Fig. 1). These structures, also referred to as 'hourglass structures' (Pattillo 1987, Woods 1988), occur on a range of scales, from regional seismic to outcrop, and in a variety of tectonic settings (e.g. Badley 1985, Pattillo 1987, Woods 1988, Wormald 1988, Pattilo & Nicholls 1990, Zhao & Johnson 1991, Odonne & Massonnat 1992, Woods 1992, Meier 1993). The mutually cross-cutting faults or fault sets in common with other conjugate shear structures, are believed to accommodate a pure shear bulk deformation, with slip on the opposed-dipping faults being either (i) sequential (Freund 1974, Ramsay & Huber 1987) or (ii) synchronous (Horsfield 1980). In this context, synchronous events are those occurring within time intervals which may be up to 1 Ma or greater. One of the problems in some previous interpretations of conjugates has been the implicit assumption that rock volumes between faults are rigid blocks, undergoing only translations, whereas it is now more widely accepted that inter-fault volumes generally undergo ductile strains, where ductile is a scale-dependent term. Such strain may be of especial significance adjacent to the intersection zones of conjugate structures, and will be reflected in the observed distributions of displacements on the constituent faults (Barnett *et al.* 1987). Analysis of the fault displacement variations and of the relative timing of movement on conjugate faults may therefore assist in discriminating between the sequential and synchronous models in respect of individual structures, and in understanding their origin.

To address these problems we have analyzed conjugate normal faults in seismic reflection data sets from the southeast edge of the Cartier Trough in the Timor Sea (Fig. 2 inset). Here, conjugate structures are common (Pattillo 1987, Woods 1988, Wormald 1988, Pattillo & Nicholls 1990, Woods 1992), and the mutual footwalls (i.e. horsts) of the structures have been identified (e.g. Woods 1992) as potential hydrocarbon traps. In this region of the Timor Sea, normal faults formed mainly during the Plio-Pleistocene (Pattillo & Nicholls 1990, Woods 1992) and accommodate extension associated with subduction of the Australian continent beneath the Banda Arc (Laws & Kraus 1974). Contemporary horizontal extension is NNW–SSE and perpendicular to faulting (Hillis 1991, Mildren *et al.* in press); this together with the mainly sub-horizontal nature of conjugate-fault intersections suggests that faulting is normal dip-slip. 2-D and 3-D seismic data provide no evidence for the presence of transverse structures.

Our structural analysis concentrates on seismic data from a well imaged Cenozoic sequence (ca 1.5–3.5 km thick) which is dominated by shelf carbonates (Pattillo & Nicholls 1990), and thickens northwestwards towards the Cartier Trough. In the upper parts of the sequence, faulting and sedimentation were synchronous, thus providing useful constraints on the timing of faulting. Many of the larger Cenozoic faults can be seen to have originated by reactivation and upward propagation of Late Jurassic normal faults in a poorly imaged sequence underlying the regional Early Cretaceous unconformity.

Attention has been concentrated on good quality 2-D seismic data for a 30 × 30 km area containing more than 50 conjugate structures. The data set comprises a rectangular array of seismic lines (32 dip-lines and 11 strike-lines with 0.5–1 km dip-line spacing); up to 25 horizons, and their associated faults, have been interpreted on

each line. Dip-lines trend at ca 65° to the faults which decreases the true fault dips by ca 5–10% and increases heave values by ca 10%. Fault throws vary only by up to 2% due to the obliquity of dip-lines to fault dip and are therefore used in our analysis of displacements; throws on the imaged faults range from ca 10 to 400 m. Since several of the conjugates are seen on more than one seismic line, the dataset provides three-dimensional control on the geometries and displacements of the structures; this three-dimensional control represents an advance on the essentially two-dimensional nature of previous studies (e.g. Horsfield 1980, Woods 1988, Zhao & Johnson 1991, Woods 1992), and has provided some new perspectives on the geometries and kinematics of conjugate faults. These seismic data are supplemented by two additional Timor Sea 3-D seismic data sets and by previously published results of physical modelling (Horsfield 1980, Woods 1988). The natural and model conjugates together provide a basis for a new interpretation of the formation and synchronous movement on intersecting conjugate faults.

The purpose of this paper is to provide insight into two key questions regarding the development of conjugate faults. (1) How do conjugate structures form? (2) How can two intersecting fault sets move at the same time? Although the conclusions are derived mainly from seismically resolvable structures developed over geological time scales, many of the ideas may have general application to synchronous-intersecting shear structures of different types and on a wide range of scales.

GEOMETRY

Conjugate structures on seismic sections are composed of faults or fault sets which dip 55°–70° in opposite directions and either cross at or converge towards a common intersection point or zone (Fig. 1). Simple conjugates comprise only two cross-cutting faults, whereas complex conjugates comprise cross-cutting fault sets. The structures are typically 'X'-shaped in cross-section, but show some asymmetry when displacements are larger on one fault than the other. Fault intersections occur at any level within the Cenozoic sequence and intersection lines of individual conjugates are generally sub-horizontal, although a few have a pronounced (<25°), but variable, plunge and clearly cut across stratigraphy. In such cases, the conjugate geometry can also be seen on appropriate horizon maps, typically as a horst passing laterally along strike into a graben (Woods 1988). On cross-sections, individual faults often cannot be traced across the intersection zones of conjugate structures either because of the style and complexity of faulting or because of the poorer seismic resolution in these zones (Fig. 1). In many such examples a significant bend in a fault trace would be required to maintain continuity of a fault across the intersection zone. Individual conjugate structures within the Cenozoic sequence are up to 10 km long (i.e. on a strike section) and 4 km wide (dip section) with vertical extents of as much as 6–7 km.

SPATIAL DISTRIBUTION OF CONJUGATE FAULTS

Figure 2 shows two distinct ENE-striking fault sets with opposite dips. Most of the larger faults dip to the south-southeast. No fault extends across the entire mapped area, and the fault map is dominated by short (< 5 km) fault traces (Fig. 2). The average line density of fault traces with throws ≥30 m is 0.41 faults/km but on smaller scales the density varies considerably, with high values particularly in the southeast of the map area. Fault traces often overlap in en échelon fashion forming either synthetic or antithetic overlaps (Morley *et al.* 1990), and the trace lengths of the two faults forming an antithetic overlap are commonly different.

Figure 3 gives the positions of conjugate structures ($N = 80$) seen on individual seismic cross-sections. Although most frequent where fault density is highest, the conjugates are widely distributed. Individual conjugate structures are most often identified on only one or two seismic lines (i.e. they are not laterally persistent). The fault map shows that ca 80% of all conjugates are near to a tip-point of at least one of the conjugate-forming fault traces, and of these ca 60% occur between the overlapping tip regions of the two constituent faults. Serial sections of a complex conjugate, seen as an antithetic overlap on the map (Fig. 3), show a progressive change in symmetry along the length of the structure (Fig. 4).

We have discriminated between conjugates in terms of size, complexity and symmetry in order to characterise better the relationships between their geometries and locations. Conjugates have been classified as either large or small structures according to whether or not they extend over a stratigraphic interval greater than the average thickness of the faulted Cenozoic sequence (ca 1.5 km). At the resolution of the fault map (Fig. 3) small conjugates occur almost exclusively either in the overlapping tip regions of the constituent faults where the overlap is identified on only one seismic line, or on small faults which are themselves seen only on a single seismic line. In contrast, large conjugates are commonly far from the tip-points of both constituent faults, individual structures intersect at least two seismic lines and their principal faults extend downwards below the Early Cretaceous unconformity. In the case of the widest and longest (ca 10 km) conjugate structure within the map area, the principal faults are extensions of much larger displacement Jurassic faults and formed by reactivation of the earlier structures. The difference in overlap lengths between small conjugates and those large conjugates which do not connect with basement structures, suggests that small conjugates can grow into larger conjugates as the lateral overlap of the constituent faults increases with fault growth. Conjugate complexity increases with size with ca 90% of simple conjugate struc-

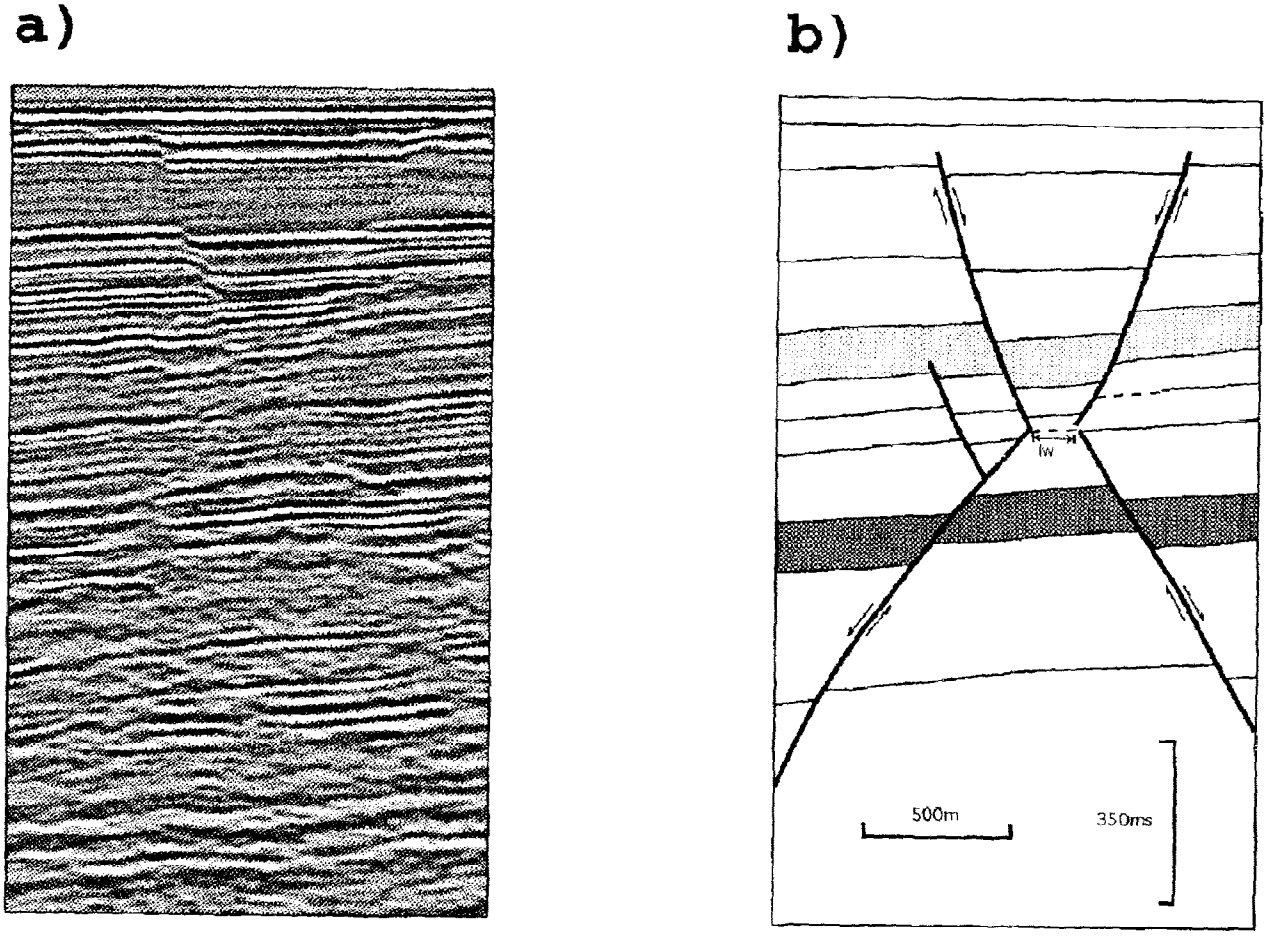

Fig. 1. Seismic section (a) and line drawing (b), on the same scales, of conjugate faults from the Timor Sea. Vertical and horizontal scales are approximately equal. Iw = conjugate intersection width. Dashed horizons are poorly resolved which within the intersection zone probably reflects a high density of sub-seismic faults.

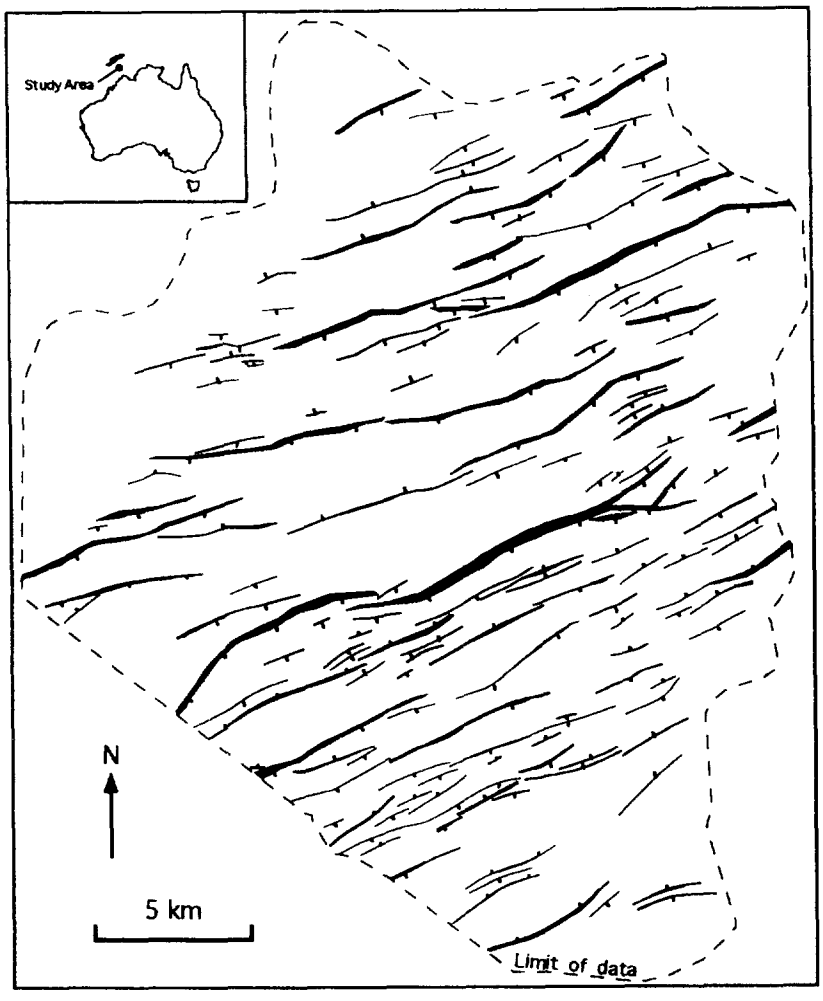

Fig. 2. Fault map for a pre-faulting lower Miocene horizon (horizon 4 on Figs. 4 and 5) in a 30 × 30 km area of the Timor Sea. Fault trace thickness is proportional to fault heave and ticks indicate downthrown sides. Inset shows location of study area.

tures classified as small and ca 80% of complex structures classified as large. Although this relationship undoubtedly reflects an evolutionary trend, it may partly be due to the failure to resolve seismically any minor faults which may be associated with small conjugates.

The distinction between symmetric and asymmetric conjugates is based on whether or not displacements at one horizon are equal on the opposed faults or fault sets: each type is present in about equal proportions. Asymmetric conjugates can occur either close to the tip-points or close to the centres of fault traces: four of the six conjugates occurring on two or more seismic lines show a change in symmetry along strike. These changes reflect lateral variations in the dip-parallel dimensions of the fault traces and in the throw on them (Fig. 5).

DISPLACEMENT ANALYSIS

Evidence concerning the interactions between the opposed-dipping faults which form conjugates and their relative timing, is likely to be preserved in the patterns of displacement variation on the fault surfaces. Fault throws within the well-imaged Cenozoic sequence were recorded as two-way travel time (TWT) differences between footwall and hangingwall cutoffs (1 ms TWT ≈ 1.4 m). The TWT/distance relationship is not strictly linear because of the velocity variations, but variations are within ±5% giving an acceptable precision for analysis of displacement variation. Detailed displacement analysis has been confined to faults in the upper part of the faulted sequence where the quality of the seismic data is highest: consequently most of the data presented are from the graben rather than the underlying horsts.

Many of the smaller faults have maximum throws within the Cenozoic sequence, whereas faults rooted in Late Jurassic structures have throws which decrease upwards within the Cenozoic sequence. Both types of displacement variation are illustrated by a fault which is an entirely Late Cenozoic structure along part of its length (Fig. 6, left), but elsewhere is rooted in a reactivated Late Jurassic fault (Fig. 6, right). On many faults, offsets of syn-faulting units towards the top of the Cenozoic sequence show rapid upward decreases which are a reflection of stratigraphic growth in the hangingwall units. Many of the faults wholly within the Cenozoic sequence show throw variations which are similar to those shown in Fig. 6 (left), whereas conjugate fault traces are significantly different with displacements decreasing towards their intersection zones.

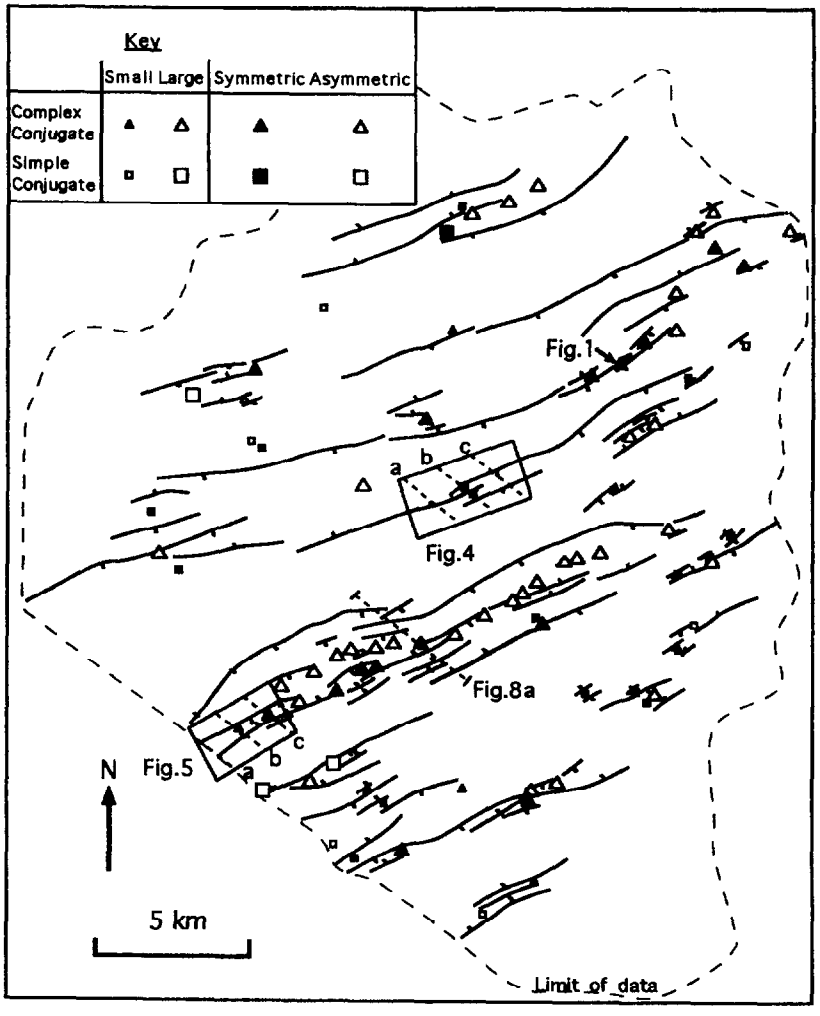

Fig. 3. Simplified version of fault map shown in Fig. 2 with fault traces shown in centre-line format. Only faults associated with conjugate structures are shown, together with locations of conjugates identified on individual seismic cross-sections (see key for details). Conjugates are represented either as horsts or as grabens, according to the depths of their intersection lines relative to the depth of the mapped horizon. Location of Figs. 1, 4, 5 and 8 are also shown.

Displacement profiles

Throw variations, as seen on cross-sections, on both simple and complex conjugate structures are shown as normalized throw profiles (Fig. 7), in which throws on principal fault(s) are plotted as a function of distance from the conjugate intersection point or zone. The distances plotted are normalized with respect to the distance between the intersection point and the upper tip-point on the fault trace. For faults which extend upwards into the syn-faulting sequence, notional tip-point positions were calculated from the displacement

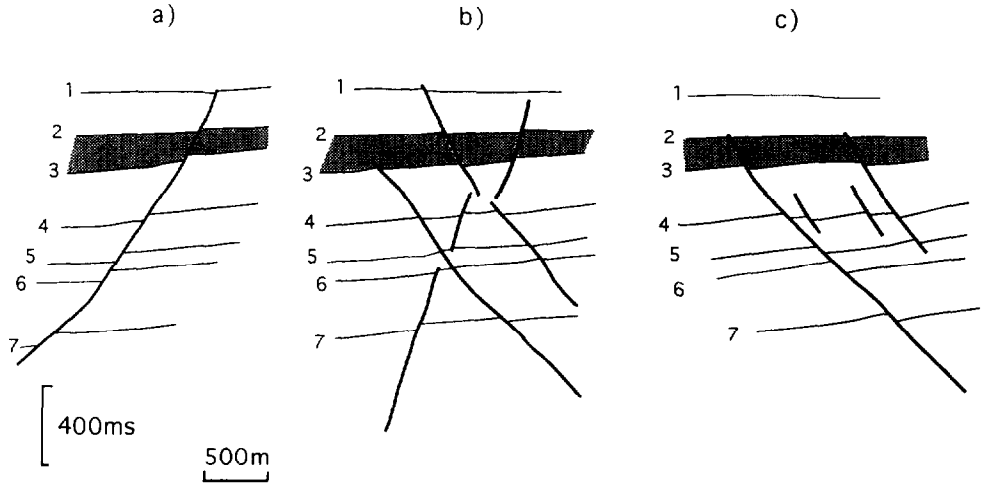

Fig. 4. Cross-sections (a–c) illustrating the along-strike change in geometry of a conjugate structure between the overlapping tips of three faults (see Fig. 3 for location). Vertical and horizontal scales are approximately equal.

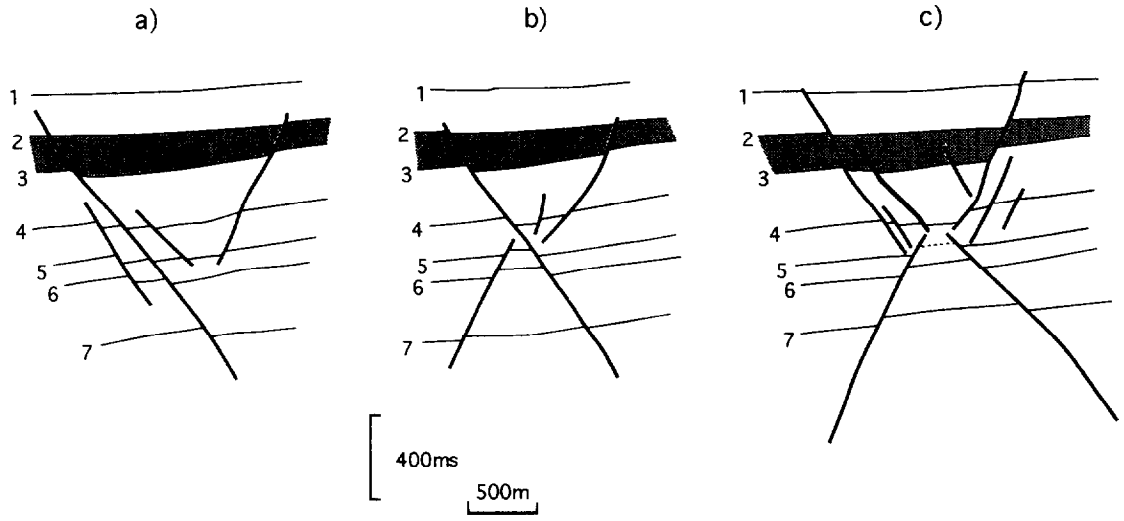

Fig. 5. Cross-sections (see Fig. 3 for location) illustrating the along-strike changes in geometry of a conjugate, from (a) opposed-dipping faults which do not intersect, to (b) an asymmetric conjugate, to (c) a complex symmetrical conjugate. The conjugate structure is only symmetrical on one section (c), mid-way along its length. Note thickening of hangingwall sequences associated with faults which intersect horizons 1–3 (stippled interval in sections b & c) indicating synchronous movement on these faults. Mutual offset of opposed fault sets across the intersection zone in section (c) also indicates synchronous movement. Vertical and horizontal scales are approximately equal.

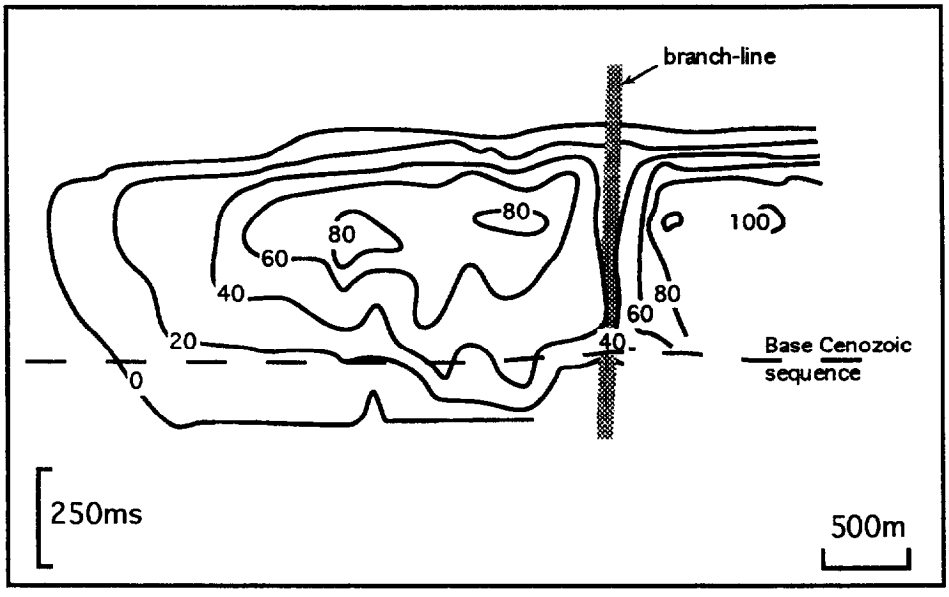

Fig. 6. Strike-projection showing variations in throw on a fault surface interpreted from a Timor Sea 3-D seismic data set (50 km south of the fault map area). Two halves of the fault are separated by a vertical region of low throws which marks the position of a branch-line (stippled) to a fault splay which strikes at ca 30° to the fault. To the left of the branch-line the maximum displacement and most of the fault surface are within the Cenozoic sequence. To the right of the branch-line the fault surface extends beyond the lower limit of the diagram into the Permo-Triassic sequence; this segment of the fault was initially formed during the Late Jurassic and reactivated and propagated upwards during the Late Cenozoic.

gradient in that part of the pre-faulting sequence lying above the point of maximum throw on the fault trace. Aggregate throw profiles for conjugate arrays (e.g. Figs. 5c and 8a) were derived by summing throws on the several faults in an array along a normal to the fault traces, as opposed to summing along an horizon. The throw data analyzed are from symmetrical conjugates only and represent the best ca 25% of the total potential data.

Simple conjugates. Small faults which are not components of conjugate structures have maximum displacements close to the mid-points of their traces on cross-sections. Throw profiles for fault traces which are components of simple conjugates are characteristically skewed towards their intersection points (particularly Figs. 7a, b & d), i.e. with maximum throws closer to the intersection points than to the upper tip-points. These faults often show a marked decrease in throw values close to intersection points, and on many faults displacement tends to zero at the intersection point. Throw gradients between points of maximum throw and intersection points (0.1–0.3 m m^{-1}) are consequently up to 2–3 times higher than those between points of maximum displacement and upper tip-points (0.05–0.15 m m^{-1}). Displacement profiles for conjugate faults generated in a

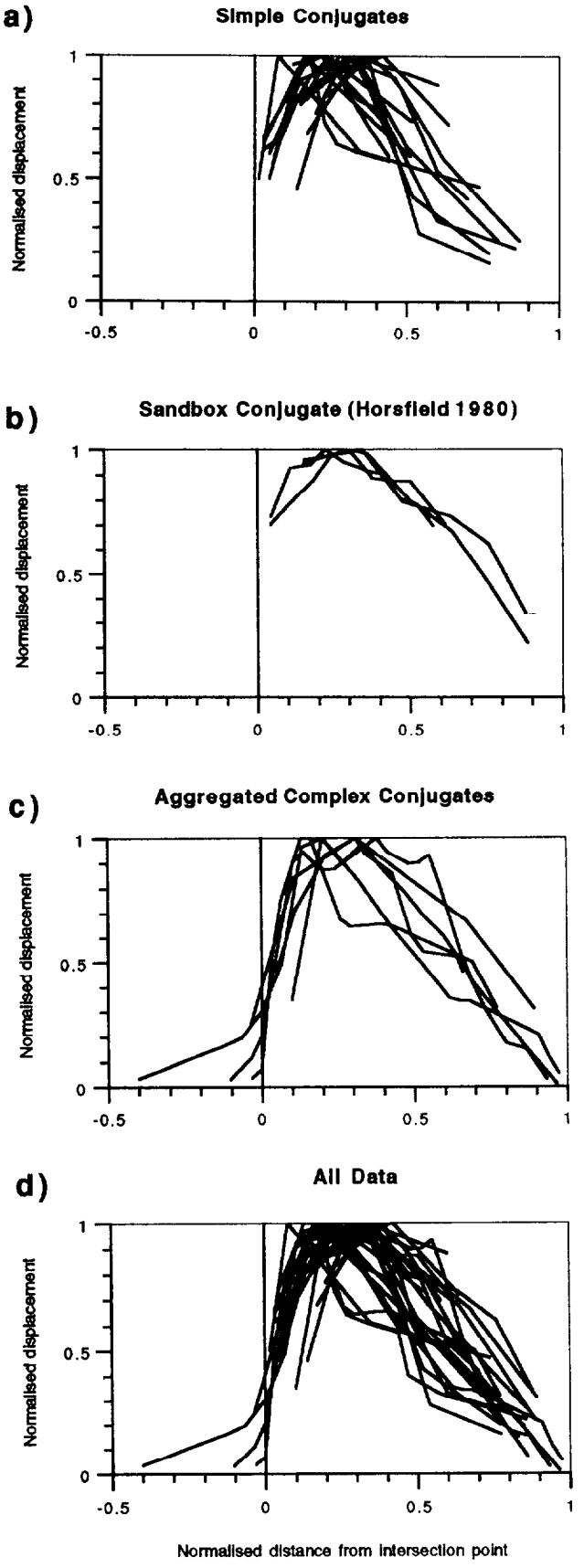

Fig. 7. Fault displacement profiles. Throws normalized to maximum throw on each fault and distances normalized to distance (along the fault) between the conjugate intersection and the fault tip (0 = intersection, 1 = fault tip). Profiles are for: (a) seismically imaged simple-conjugate structures (14 profiles); (b) a sandbox simple-conjugate structure from fig. 3(a) of Horsfield (1980) (4 profiles); (c) aggregated complex-conjugate structures (6 profiles); and (d) all data. Note the asymmetry of the profiles towards their intersection zones.

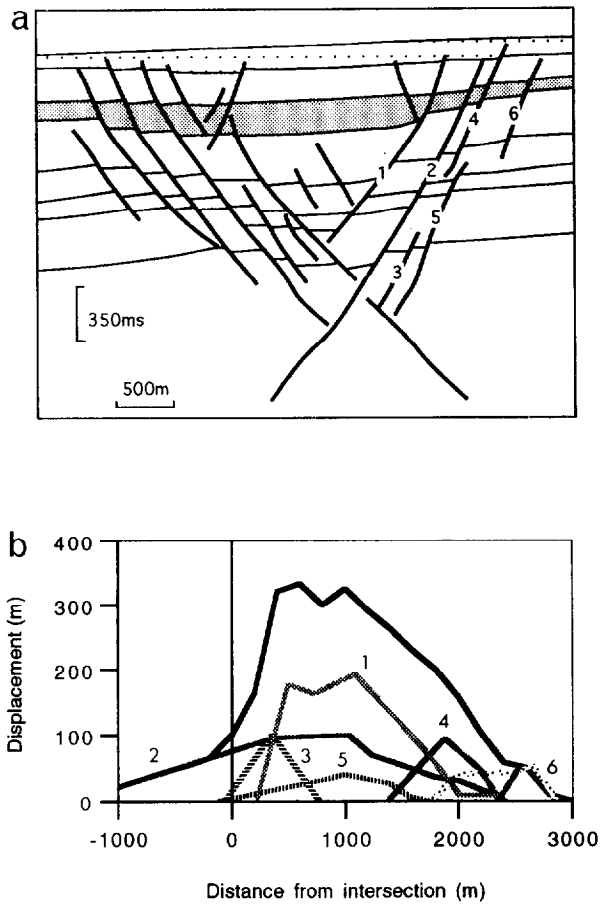

Fig. 8. (a) Cross-section of a complex conjugate drawn from seismic data (see Fig. 3 for location). Faulting and sedimentation were synchronous in and above the lowest shaded unit. Vertical and horizontal scales are approximately equal. (b) Displacement profiles of numbered faults shown in (a) and their aggregate profile (bold line).

physical model (Horsfield 1980, Fig. 7b) have geometries similar in many respects to those of the Timor Sea structures. The modelled faults have displacements which decrease both towards the conjugate intersections, as with their natural counterparts, and towards the edges of the sandbox due to the model boundary effects. Although most obvious in the early stages of model fault development, throw decreases towards conjugate intersections are characteristic of the incremental displacements at all stages of growth. Decreasing throws towards conjugate intersections are a positive indication that the inter-fault volumes in both natural and model systems have undergone significant ductile strain (see *Strain Data* section).

Complex conjugates. Figure 8(b) shows aggregate displacement profiles for a large complex conjugate (see Fig. 3 for location) composed of 20 faults (Fig. 8a). Displacement profiles for the individual fault traces on the right-hand side of the conjugate, labelled 1–6, have been summed to produce an aggregate profile (Fig. 8b). Although these faults often do not individually show the asymmetry typical for faults in simple conjugates (Figs. 7a & b), their aggregate profile is very similar to profiles of individual faults in simple conjugates. The highly ordered form of the aggregate profiles and their simi-

larity to profiles of single faults in simple conjugates testify to a high degree of geometric and kinematic order in this complex conjugate. Kinematic coherence in normal fault arrays in the North Sea is believed to have required a high degree of overlap between the time intervals during which individual faults were active (Walsh & Watterson 1991). A similar conclusion for the Timor Sea fault arrays is supported by their relationships with syn-faulting stratigraphic units (see *Timing of Faulting* section).

Since the displacement profile data (Fig. 7) are derived from both simple and complex conjugate faults of varying dimensions and maximum displacements, from both seismically imaged structures (Figs. 7a, c & d) and sandbox model faults (Horsfield 1980, Fig. 7b), it can be concluded that the characteristic profile is independent of scale. This observation suggests that throughout growth of an individual fault, and of the conjugate structure of which it is a part, the displacement profile maintains a similar form. Persistence of a skewed displacement profile throughout growth of a fault requires progressive migration of the maximum displacement along the fault trace away from the intersection point. The skewed profile could arise from progressive changes in the proportions of slip accommodated by the seismically imaged fault zone on the one hand, and by ductile deformation on the other (see next section).

STRAIN DATA

Displacement variations on fault traces parallel to the slip direction are accommodated by volumetric strains in the rock volume surrounding the fault (Barnett *et al.* 1987). On cross-sections of normal faults these volumetric strains are expressed as positive or negative linear strains adjacent and parallel to the fault traces. Higher displacement gradients require higher strains, and the maximum strain is expected in the hangingwall of a normal fault because more of the displacement on a normal fault is accommodated by hangingwall subsidence than by footwall uplift (Gibson *et al.* 1989, King *et al.* 1989). The strains can be assessed by quantifying thickness changes of individual stratigraphic units across a fault by calculation of a growth or strain index, as follows:

$$\text{Growth/strain index} = (HW - FW)/FW,$$

where HW and FW are the thickness of a stratigraphic unit in the hangingwall and footwall of a fault, respectively. In a pre-faulting sequence this index is an indirect measure of strain, whereas in a syn-faulting sequence it is a function of both the strain and of the relative rates of sedimentation and faulting. Growth-strain indices from two Timor Sea data sets, including the main study area, and from a physical model of conjugate faults (Woods 1988) have been plotted (Fig. 9) as a function of the vertical distance from the intersection zone. The resulting curves have three distinct segments. (i) Near the intersection the growth-strain indices are negative, indicating relative thinning of the hangingwall units. Indices approach zero with increasing distance from the intersection point. (ii) The central portion of the plot is characterised by low, generally negative, indices. (iii) High positive indices correspond to those parts of fault traces which are in the syn-faulting sequence.

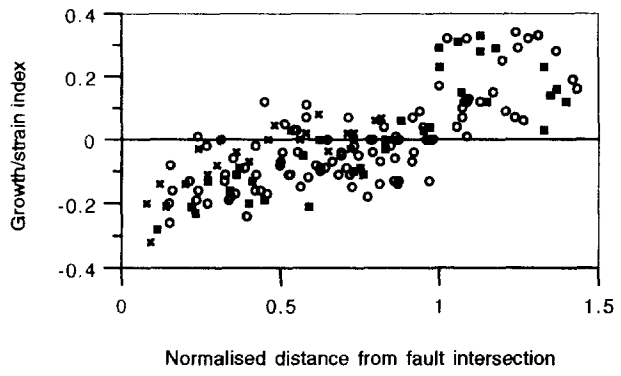

Fig. 9. Growth/strain index (=$(HW - FW)/FW$) vs normalized distance from the conjugate intersection zone. Distance is normalized with respect to the vertical distance between the intersection point and the base of the syn-faulting sequence. Data (N = 176) are from the map area of Fig. 2 (filled squares), a second seismic data set from the Timor Sea (open circles) and a sandbox model shown as fig. 6(b) in Woods (1988) (crosses).

The data indicate up to 20–30% thinning in hangingwall sequences between fault traces near conjugate intersection zones (Fig. 9); within the limits imposed by the resolution of the seismic data, thinning occurs uniformly across the mutual hangingwall of the conjugate structure. Thinning directly reflects the high displacement gradients in these regions. Sandbox experiments (Horsfield 1980, Woods 1988) accommodate conjugate formation by horizontal extension at the fault intersection with no significant difference between pre- and post-deformational cross-sectional areas. However, Odonne & Massonnat (1992) record high vertical shortening strains associated with both model conjugate faults in paraffin wax and conjugate faults in a Cretaceous Flysch outcrop, from which they conclude that volume loss by pressure solution can occur to accommodate movement on the faults. It is evident that the geometrical consequence of displacements which reduce towards the intersection points to conjugates, at which displacements may be zero, could be accommodated either by horizontal extension or by volume loss. Which of these alternatives applies in a particular case must depend mainly on the material properties and on the rate of fault growth, and possibly on the scale. As the Cenozoic sequence in those parts of the Timor Sea from which our data derive is dominated by shelf carbonates, volume loss by pressure solution cannot be discounted.

Inspection of cross-sections of simple conjugates shows that the intersection point of the principal faults forming one side of a conjugate does not coincide with the intersection of the principal faults forming the other side. The horizontal distance between the two intersection points is the intersection width (Fig. 1) which, assuming originally straight bounding faults, provides an indirect measure of ductile strain within the intersection

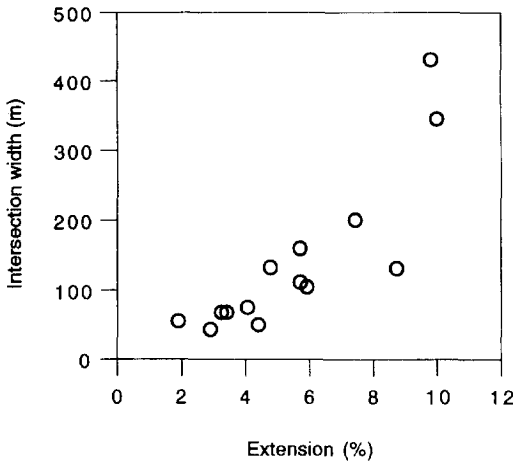

Fig. 10. Plot of conjugate intersection width (defined in Fig. 1) vs the maximum extension (%) shows a positive relationship between the two variables. Maximum extension is measured from the horizon most extended by seismically imaged faults and is calculated by dividing the aggregate heave by the horizon length within the conjugate structure. Data ($N = 14$) are from the map area shown in Fig. 2.

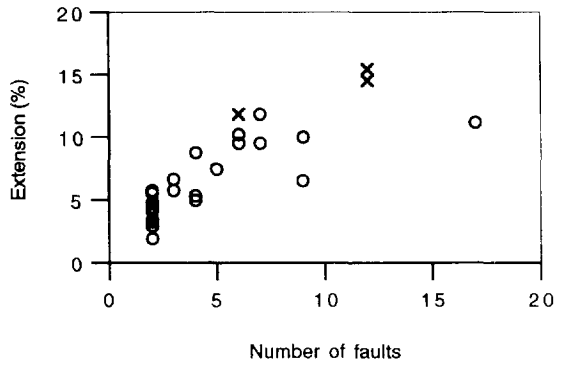

Fig. 11. Plot of maximum extension (%) vs the total number of seismically imaged faults above the intersection zone for 26 conjugates from the Timor Sea. Maximum extension is measured from the horizon most extended by seismically imaged faults and is calculated by dividing the aggregate heave by the horizon length within the conjugate structure. The data are all from the Timor Sea and include structures from this study (closed circles) and Woods (1988) (crosses).

zone. Figure 10 shows that intersection width generally increases with the maximum extension, which is measured for the horizon most extended by seismically imaged faults across the conjugate. For individual conjugates the increase in intersection width equates approximately with a decrease in the throw accommodated by seismically imaged faults in and adjacent to intersection zones.

Complex conjugates consist of numerous individual faults and the relationship between the number of faults and the extension associated with individual structures has been examined. The maximum fault-related extension (%) is plotted against the total number of seismically imaged faults above the intersection zone for 26 conjugate structures (Fig. 11). For simple conjugates consisting of only two faults, extension estimates range from ca 2 to 6%. As the number of faults increases, measured extensions increase to about 15% in an approximately linear fashion (Fig. 11). These data are consistent with the progressive growth of a conjugate structure, as reflected by increasing extension, being complemented by increases in fault numbers and in complexity. Although similar changes occur in the model conjugates described by both Horsfield (1980) and Woods (1988), model structures with geometries comparable to those of the natural structures show extensions 2–4 times greater than those associated with their natural counterparts.

TIMING OF FAULTING

Two types of data can be used to investigate the relative timing of movement on opposed-dipping conjugate faults in the Timor Sea data sets: (i) stratigraphic evidence from syn-faulting sequences and (ii) geometries of cross-cutting faults. Our main concern is to establish whether fault movements on opposed-dipping faults or fault sets are synchronous or are sequential. If faults dipping in one direction are consistently offset by, and therefore older than, opposed-dipping faults, then no geometric or kinematic problem arises. By contrast, synchronous movement on cross-cutting conjugate faults presents significant problems concerning compatibility of geometries and strains in the vicinity of the intersection zone.

The geometry of the conjugates provides indirect evidence for the timing of faulting. In many cases (e.g. Fig. 1) the cross-cutting faults mutually offset each other, indicating synchronous fault movements; an intersection width would not exist if movement on the bounding faults were sequential. Since most seismically resolved conjugate structures in the Timor Sea data sets extend upwards into the mainly Plio-Pleistocene (Woods 1992) syn-faulting sequence, stratigraphic evidence also is available for the timing of fault movements. Time resolution is no better than the intervals corresponding to deposition of the seismically resolved stratigraphic units (100–300 m thick), deposited over time intervals averaging ca 1 Ma. Within individual conjugate structures all faults appear to have remained active until approximately the same time, as indicated by the similar stratigraphic level within the syn-faulting sequence of their upper tip-points (see Figs. 5 and 8a). Stratigraphic growth of syn-faulting hangingwall units is associated with all faults, but is more subdued for small displacement faults than for larger displacement faults. Differences in times of initiation of faults within an individual conjugate structure have not been detected on the basis of differences in the stratigraphic levels at which hangingwall growth first started. However, the failure to identify different ages of initiation of individual faults must be due to the limited time resolution of the data as complex and wider multi-fault conjugates have developed from simpler structures. As the largest faults in a conjugate array tend to be the innermost faults, it is likely that the increase in numbers of faults which accompanies conjugate growth is achieved by growth of

new faults in the external parts of the arrays. By contrast, in the modelled conjugates (Horsfield 1980, Woods 1988) the new faults added as conjugates become more complex are concentrated in the internal parts of the structures.

ORIGIN OF CONJUGATE STRUCTURES

A crucial question concerning conjugate structures is whether they form by the incidental intersection of independently nucleated opposed-dipping faults or by nucleation and growth from an intersection point. As conjugate structures are often approximately symmetrical in cross-section, it may be tempting to conclude that they are intrinsic structures that originate as single kinematic units, with upward and downward propagation from their intersection points. If this is the case, the structures would also be expected to be approximately symmetrical in three dimensions. Symmetry in three dimensions would require that conjugate fault pairs would have comparable lateral extents and locations and matching positions of maximum displacement, i.e. on a map, a normal to the parallel fault traces would pass through the points of maximum displacement on both traces.

On the map (Fig. 3), conjugate structures are seen not to be associated with symmetrically disposed fault trace pairs, but rather with pairs of fault traces of different sizes and lengths which are not symmetrically disposed with respect to one another. Many conjugates occur at antithetic overlaps between opposed-dipping faults, showing a change in symmetry along the length of the overlap, and are more easily accounted for by incidental intersection primarily due to lateral fault propagation. The widest and longest (10 km) conjugate structure, by contrast, is bounded by faults which represent the upward extension of larger displacement Jurassic faults, and formed by reactivation and upward propagation of the earlier fault surfaces. From the map (Fig. 3), it can be seen that for most faults which form parts of conjugate structures, the greater part of each fault surface is not a part of a conjugate, the same is also true for conjugates bounded by the uppermost extension of reactivated Jurassic faults. These observations, together with the wide but irregular distribution of conjugate structures, are consistent with them having been formed by the incidental intersection of two independent faults, or fault arrays, with opposing dips.

In the general case of intersection of two growing, ideally elliptical, fault surfaces, the direction of propagation of each of the two faults at the initial point of intersection will be normal to the local tip-lines of the faults. In the Timor Sea, however, the intersections appear to be due predominantly to either lateral or up-dip growth. The preponderance of these two relatively simple types of intersection is believed to be due to the fact that the faults originated in one of two ways, i.e. either by nucleation within the Cenozoic sequence or by upward propagation of Late Jurassic faults. Two faults nucleated within the Cenozoic sequences are likely to intersect at laterally propagating tip-lines and faults propagating from the Jurassic are likely to intersect by up-dip propagation. In the few cases ($N = 16$) where the tip-lines for isolated faults have been mapped, the fault surfaces have aspect ratios of about 2:1, with the long dimension horizontal. Lateral propagation rates are therefore likely to be about double those of dip-parallel propagation rates, which is likely to increase the incidence of lateral intersections.

There is a basic difference between intersection by lateral propagation and intersection by dip-parallel propagation. In the case of lateral propagation, the intersection originates by intersection of tip-lines and further growth of both faults lengthens their intersection line which locally separates each fault surface into two lobes (Fig. 12). In the case of intersection by dip-parallel propagation it is unlikely that both tip-lines will reach a potential intersection point at the same time, and the initial intersection will be between a tip-line and some point on the fault surface of the opposed-dipping fault. In this second case the propagation of the tip-line may be stopped, or at least interrupted, by the surface of the opposed-dipping fault and 'T' or 'Y' junctions are likely to occur. A further difference between the two cases is that when intersection by lateral propagation has occurred, the intersecting parts of the two faults will have similar throws and trace lengths on the cross-sections containing the intersection. In these cases the conjugate will be symmetrical in the early stages and as the intersection line lengthens the conjugate will remain approximately symmetrical at the centre of the overlap and will be asymmetric towards the ends. Conjugates interpreted to have formed in this way are relatively short structures, usually not more than 2–3 km long, although longer overlaps are generally associated with larger displacement bounding faults. Intersections formed by dip-parallel propagation are less likely to be symmetrical because the two faults do not meet at a point where their displacements are the same. For example the largest conjugate in the study area (see Fig. 8) is dominated by one of the fault pair.

The origin of Timor Sea conjugate structures is attributed to incidental intersection of opposed-dipping faults in which the dimensions, locations and displacement patterns of the future conjugate-fault pairs were unrelated. The conjugates are not intrinsic structures formed by propagation from their intersection point. Following their intersection, the geometric development of each fault is strongly influenced by slip on the other, at least within the local volume where they have intersected (Fig. 12; see below). A high proportion of the surfaces of the two intersecting faults is remote from the intersection, particularly when they first intersect. This feature is significant when the question of synchronous movement is considered. A conjugate structure is unlikely to become mechanically locked when only small parts of its constituent fault surfaces are within the conjugate structure.

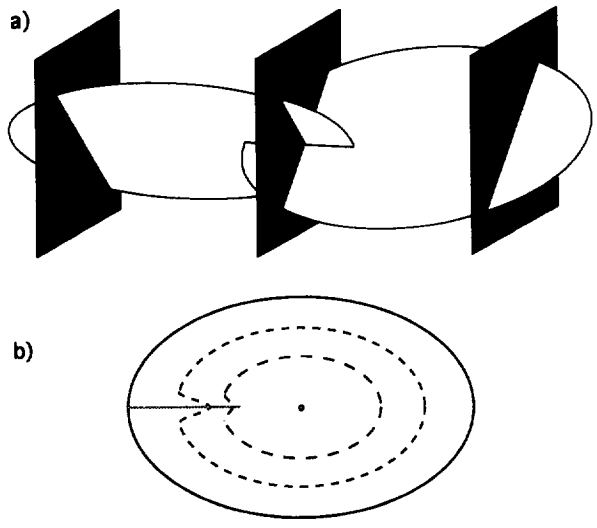

Fig. 12. (a) Schematic three-dimensional diagram showing the geometry of a conjugate developed between the overlapping lateral tips of two elliptical opposed-dipping faults. The conjugate structure exists only in the overlap region and changes from asymmetric towards the edges of the overlap to being approximately symmetrical towards the middle. (b) Shows throw contours on one of the conjugate faults which decrease close to the conjugate intersection zone (marked by a horizontal line).

Occurrence of conjugate structures

If conjugate structures are, as we believe, formed by the incidental intersection of two opposed-dipping fault sets, then they might be expected to occur more commonly in other areas of normal faulting than appears to be the case. Using the map (Fig. 2) and making the assumption that all adjacent faults with opposed dips will intersect, either above or below the mapped horizon, it is estimated that conjugates should be four times more abundant in this data set than they actually are. There are three principal reasons why immediately adjacent opposed-dipping faults do not provide conjugate structures. (i) One or both faults terminate either up or down dip before they intersect. (ii) Opposed-dipping faults abut at a 'T' or 'Y' junction but do not cross-cut. (iii) The potential intersection is either above or below the vertical limits of the seismic data in which faults are well imaged. In spite of these factors, conjugates are still relatively common in the study area.

The factors likely to govern the frequency of conjugate structures include the fault density, the typical vertical extent of faults, the relative number and spatial distributions of faults in the opposed-dipping sets and the vertical extent of the imaged sequence; some of these attributes are strongly dependent on the quality and resolution of the seismic data. To illustrate the relative importance of these factors a comparison has been made between the Timor Sea data set and a typical North Sea data set with few conjugates (see Table 1). Although the North Sea survey area is approximately twice that of the Timor Sea survey, only 10 conjugates are observed, i.e. an eighth of the Timor Sea conjugates. The data sets are similar in respect of the vertical ranges of the imaged sections, the average vertical extents of the faults and in the proportions of opposed-dipping faults. In many other North Sea data sets the vertical extent of the imaged sections is <500 m (e.g. Abbotts 1991), and the likelihood of observing an intersection of opposed-dipping faults is correspondingly lower. Significant differences between the Timor Sea and North Sea data sets are in respect of average fault density, seismic resolution and the spatial distribution of opposed-dipping faults (Table 1). A further difference is in the numbers of distinct acoustic boundaries within a given vertical interval; the number of mappable reflections in the Timor Sea data set is unusually high and the conjugates structures are correspondingly prominent.

The fault density for throws of ≥30 m is 60% higher in the Timor Sea data set than in the North Sea example. In the Timor Sea faults are therefore more closely spaced and more likely to intersect within a given vertical interval by a factor of ca 1.6.

The vertical seismic resolution for the North Sea data set (≥30 m) is approximately twice that of the Timor Sea data set (≥15 m), which affects both the relative numbers of observed faults and the dimensions of the fault surfaces in the two data sets. In the North Sea data set many faults with maximum throws of <30 m are not seismically imaged, while on larger faults (i.e. with a maximum throw >30 m) the tip regions with throws <30 m may not be represented. The underrepresentation of tip regions with throw <30 m in the North Sea data set is confirmed by the higher median throws for similar average fault vertical dimensions relative to faults in the Timor Sea (Table 1). Although conjugate structures do occur in the North Sea data set, their frequency may be underestimated because of the poorer seismic resolution. If the seismic resolution of the Timor Sea data set were to be degraded to that of the North Sea data set we estimate that only ca 50% of the currently observed conjugates would be identified.

Another important attribute affecting the numbers of conjugates seen in these data sets is the average number of consecutive faults with the same dip direction ('distribution of opposed-dipping faults' in Table 1). Fault intersection is most likely when this number is unity and all pairs of adjacent faults have opposed dips. The data in Table 1 show that adjacent faults dipping in opposed direction are more common in the Timor Sea data set and this difference is directly reflected in the higher number of observed conjugates.

The difference between the two data sets in the occurrence of conjugate faults is therefore due not only to the limitations of the method of observation, in respect of both seismic resolution and the depth interval imaged, but also to the spatial distribution of faults. The likelihood of conjugate faults being seen in a data set is therefore due not only to observational factors but also to the spatial systematics of the faults, which may reflect fundamental differences in the mechanical conditions under which they formed.

Table 1. Fault attributes of a typical North Sea seismic data set compared with those of the Timor Sea data set. The 'distribution of opposed-dipping faults' gives the mean number of adjacent faults dipping in the same direction encountered on dip lines.

Data sets		North Sea	Timor Sea
Fault density	Range (faults/km)	0.07–0.46	0.12–0.71
	Average (faults/km)	0.25	0.41
Median throw (m)		40	26
Seismic resolution (m)		30	15
Vertical extent faulting (m)		1800	1600
Average vertical fault dimension (m)		1000	850
Ratio opposed-dipping faults (%)		46:54	35:65
Distribution opposed-dipping faults		2.6	1.7
Conjugate Structures	No.	10	80
	No./100 km	0.6	10

KINEMATIC MODEL FOR CONJUGATE INTERSECTION ZONES

The distinction between sequential and synchronous movement on intersecting faults sets is important because it has a bearing on wider questions concerning pure vs simple shear strain of the crust, non-plane strain crustal deformation by faulting and the polarization of fault systems. For example, would the existence of two intersecting fault sets lead to an effective strain hardening of crust because of each fault set locking the other? If so, how would a general strain be accommodated?

We follow Horsfield (1980) in arguing that sequential movement of opposed-dipping faults or fault sets, i.e. with displacement on one fault completed before movement on the other begins, cannot give rise to conjugate structures of the type we have described. Where sequential movement on two or more fault sets has occurred the chronologic sequence should be simple to determine given adequate data (e.g. Zhao & Johnson 1991) and no special geometric or kinematic problem arises. Suggestions that conjugate relationships are necessarily sequential (e.g. Freund 1974, Jackson & McKenzie 1983, Ramsay & Huber 1987) appear to be based on the assumption that synchronous movement on intersecting faults is not possible, even though the feasibility of synchronous movement on other types of opposed-dipping intersecting shear structures, e.g. kink-bands (Anderson 1974) and shear bands (Platt & Vissers 1980), appears to be accepted without question.

Although the time resolution of the Timor Sea seismic data is poor relative to the likely intervals between individual slip events on a fault, it is good relative to the active lifetime of a fault. Movements on intersecting pairs of faults, or fault arrays, overlapped to an extent which justifies conjugate pairs being described as synchronous. On the time scale of individual slip events, movement on the conjugate pairs may well have been alternating and a compatible geometry which could result from a small number of alternating slip events is shown in Fig. 13(b). Within the intersection zone, which widens with each slip event, the cumulative displacement is distributed between several individual slip surfaces rather than concentrated on a single surface, with a new slip surface generated for each slip event. Each new slip surface connects the two principal fault lobes, above and below the intersection zone, to form a single non-planar slip surface for each slip event. Although slip can take place on a non-planar surface, the radius of curvature of the bends in the slip surface is a limiting factor. To remain within this limit, each new slip surface intersects the principal lobes of the faults at points progressively more distal from the original intersection. This progressive change has two effects. The first is to increase the vertical thickness of the ductile intersection zone. The second effect is the bypassing of the proximal parts of the principal fault lobes so that these parts become inactive and the points of maximum displacement become progressively more distal from the original intersection. These changes are seen on seismic sections as decreases in the displacement on the principal fault surfaces towards the intersection zones. In practice, the aggregate displacement does not decrease towards the intersection but progressively smaller proportions are accommodated on the seismically imaged main fault surfaces and progessively greater amounts are accommodated on dispersed slip surfaces and seen as ductile strain. The contrast between those parts of a fault where slip is concentrated on a single surface, or within a discrete fault zone, and those where the slip surfaces are dispersed leads to an observed structure as shown in Fig. 13(c). As each fault may have grown in some thousands of slip increments it is unlikely that the regular geometries of the type shown in Fig. 13(b) will be maintained, but the intersection zone will be characterized by a complex network of intersecting slip surfaces, each accommodating a small amount of slip. Marker surfaces passing through the intersection zone will be displaced by numerous small opposed-dipping faults and will not show vertical offsets on seismic sections, on which they will appear to be extended horizontally and thinned vertically. When it is recalled that the two discrete lobes of a fault on either side of an intersection zone often represent only a small proportion of the whole fault surface, and that these lobes are connected primarily through their continuity with that part of the fault surface lying beyond the conjugate structure, there is no mechanical requirement for them to be connected through the intersection zone by a single slip surface even during a single slip increment.

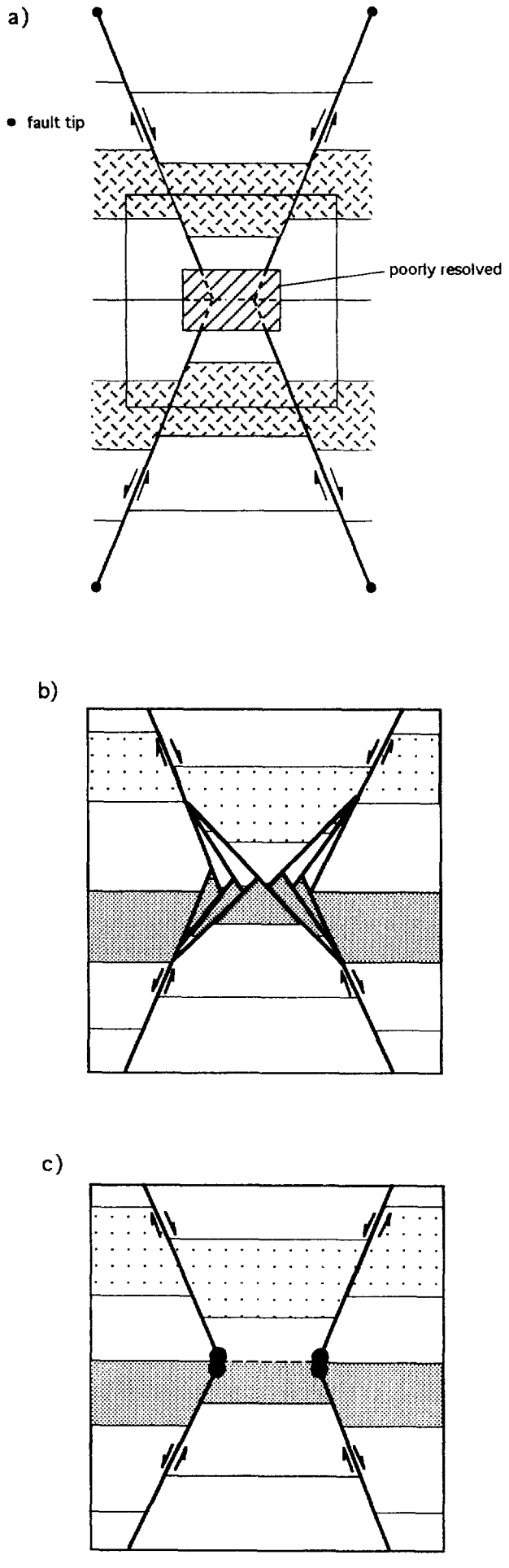

An interpretation of this type serves to emphasize that the concept of 'brittle' deformation with rigid blocks translated along faults is, at best, valid only for the microscopic scale. With any method of observation which does not image the smallest faults, the effect of faults below the limit of resolution of the observation method will be seen as ductile strain of the material between the imaged faults. Processes other than faulting (e.g. pressure solution) may also contribute to ductile deformation, but appear not to be essential in the formation of synchronous intersecting conjugate faults.

DISCUSSION

The confirmation that intersecting faults can move synchronously without mechanically locking the system removes any doubt that an appropriate range of fault orientations can accommodate a general deformation of the crust (Reches 1978), although it is possible that temporary mechanical locking can occur locally when faults intersect at a tip-line/fault surface junction as opposed to a tip-line/tip-line junction.

The incidental and random formation of the conjugate structures in the Timor Sea emphasizes that conjugate structures are not a requirement for pure shear deformation of the crust, as this can be accommodated by two or more fault sets even when, on the scale of observation, they are not seen to intersect. On the other hand, where evidence from syn-faulting sedimentation is not available, the existence of a conjugate of the type described would demonstrate the synchroneity of the intersecting fault sets.

Other types of conjugate shear structures, such as ductile shear zones and kink-bands, are likely to have origins similar to those of conjugate faults in so far as they arise by incidental intersections of initially independent structures. Conjugate extensional shear bands (Platt & Vissers 1980) and other conjugate structures related to boudinage, may be different in so far as they nucleate within a particular layer and may initiate as primary conjugate structures accommodating necking. The complex Timor Sea conjugates represent large scale necking phenomena with geometries in many respects closely comparable with true necking, e.g. the layer coinciding with the symmetry plane is not offset but is uniformly stretched and layers farthest from the symmetry plane are the most offset.

What appears on a seismic scale as a ductile conjugate fault intersection zone is likely to appear on core or outcrop scale as a zone of numerous intersecting and mutually offsetting slip surfaces with a relatively small

Fig. 13. (a) Schematic diagram of a simple-conjugate with geometry, fault displacements and data resolution comparable with those of the seismically imaged structures in the Timor Sea. The box in (a) indicates the region represented at larger scales in (b) & (c). (b) Shows the structure produced by alternating slips on the conjugate faults for a small number of large slip events. (c) Shows a conjugate structure at a resolution typical of seismic data incorporating many slip events and a distributed network of sub-seismic faults in the intersection zone.

displacement on each (Fig. 13b). Heavily faulted zones of this type are expected to be preferred sites for hydrothermal alteration and mineralization. Although we know of no outcrops which have been specifically identified as representing fault intersection zones on a scale comparable with the Timor Sea conjugates, we expect such outcrops to occur.

The mutual footwall (i.e. horsts) of conjugate normal faults provide structural closures which have been recognized as potential hydrocarbon traps (e.g. Woods 1992). Two principal geometries may result in trap formation. Firstly, lateral variations in fault displacement, and hence footwall uplift, will result in the development of a pericline or saddle in the conjugate horst. Due to the displacement partitioning and the dominance of hangingwall subsidence these culminations will be smaller in amplitude than their complementary synclines in the conjugate graben. Secondly, where the conjugate faults differ in strike, and their line of intersection therefore is not horizontal, and where the dip direction of the stratigraphic units is opposed to the plunge direction of the conjugate intersection, there will be a potential trap in the host block, if the faults are sealing. Both types of conjugate trap may be small in horizontal dimension (<2–3 km) and laterally discontinuous. Such structures will be seismically mappable only where the seismic data are of sufficient quality below the intersection zones, which may be exceptional. On the other hand, the existence of such structures can often be inferred from the geometry of an overlying graben.

CONCLUSIONS

(1) Conjugate structures comprise two normal faults or fault sets which meet along a common intersection line and have an 'X' shape in cross-section.

(2) Conjugate structures form due to the incidental intersection of opposed-dipping faults. Factors which affect the development and subsequent observation of these structures include: the fault density, the spatial distribution of opposed-dipping faults, the seismic resolution and the vertical extent of the imaged fault data.

(3) Large conjugates grow from small structures; larger conjugates are associated with more numerous and larger faults than small structures.

(4) Many of the faults within a given conjugate structure are active synchronously on a geological time scale.

(5) Synchronous movements on intersecting opposed-dipping faults can be accommodated by reduction of displacements on discrete fault surfaces towards the fault intersection zone, and a corresponding increase in the ductile strain. The ductile strain is effected by sub-seismic faults. High strains occur in the volume proximal to the fault intersection and produce thinning and extension of the stratigraphic units between the conjugate faults.

Acknowledgements—We thank Ampolex Ltd, BHP Petroleum and Statoil for providing the seismic data on which this work is based; publication is with the permission of these companies. We are grateful to Chris Bonson and Isabel Jones for preparation of diagrams and to other Fault Analysis Group colleagues for discussions on several aspects of this work. Graham Yielding interpreted the North Sea seismic data set. This research was part funded by the OSO/NERC Hydrocarbon Reservoirs LINK Programme (project number 827/7053) and by the NERC Petroleum Earth Sciences Programme (grant D1/G1/189/03). Badley Earth Sciences FAPS software was used for correlation, projection and analysis of fault data.

REFERENCES

Abbotts, I. L. (Ed.) 1991. United Kingdom oil and gas fields 25 years commemorative volume. *Mem. geol. Soc. Lond.* **14**.

Anderson, T. B. 1974. The relationship between kink-bands and shear fractures in the experimental deformation of slate. *J. geol. Soc. Lond.* **130**, 367–382.

Badley, M. 1985. *Practical Seismic Interpretation*. Unpublished manual.

Barnett, J. A. M., Mortimer, J., Rippon, J. H., Walsh, J. J. & Watterson, J. 1987. Displacement geometry in the volume containing a single normal fault. *Bull. Am. Ass. Petrol. Geol.* **71**, 925–937.

Freund, R. 1974. Kinematics of transform and transcurrent faults. *Tectonophysics* **21**, 93–134.

Gibson, J. R., Walsh, J. J. & Watterson, J. 1989. Modelling of bed contours and cross-sections adjacent to planar normal faults. *J. Struct. Geol.* **11**, 317–328.

Hillis, R. R. 1991. Australia–Banda Arc collision and *in situ* stress in the Vulcan Sub-basin (Timor Sea) as revealed by borehole breakout data. *Explor. Geophys.* **22**, 189–194.

Horsfield, W. T. 1980. Contemporaneous movement along crossing conjugate normal faults. *J. Struct. Geol.* **2**, 305–310.

Jackson, J. & McKenzie, D. 1983. The geometrical evolution of normal fault systems. *J. Struct. Geol.* **5**, 471–482.

King, G. C. P., Stein, R. S. & Rundle, J. B. 1989. The growth of geological structures by repeated earthquakes, 1. Conceptual framework. *J. geophys. Res.* **93**, 13,307–13,319.

Laws, R. A. & Kraus, G. P. 1974. The regional geology of the Bonaparte Gulf Timor Sea area. *Australian Petrol. Explor. Ass. J.* **14**, 77–84.

Meier, D. 1993. *Abschiebungen: Geometrie und Entwicklung von storungen im Extensionsregime*. Ferdinand Enke Verlag, Stuttgart.

Mildren, S. D., Hillis, R. R., Fett, T. & Robinson, P. H. In press. Contemporary stresses in the Timor Sea: implications for fault-trap integrity. In: *West Australian Basins* (edited by Purcell, P. G. & Purcell, R. R.). *Proc. Explorat. Soc. Australia Symp., Perth*, 1994.

Morley, C. K., Nelson, R. A., Patton, T. L. & Munn, S. G. 1990. Transfer zones in the East African Rift System and their relevance to hydrocarbon exploration in rifts. *Bull. Am. Ass. Petrol. Geol.* **71**, 1234–1253.

Odonne, F. & Massonnat, G. 1992. Volume loss and deformation around conjugate fractures: comparison between a natural example and analogue experiments. *J. Struct. Geol.* **14**, 963–972.

Pattillo, J. 1987. Tectono/stratigraphic framework and structural review of permit AC/P4, Timor Sea region, BHP Petroleum Pty Ltd Report (unpublished).

Pattillo, J. & Nicholls, P. J. 1990. A tectono-stratigraphic framework for the Vulcan Graben, Timor Sea region. *Australian Petrol. Explor. Ass. J.* **30**, 27–51.

Platt, J. P. & Vissers, R. L. M. 1980. Extensional structures in anisotropic rocks. *J. Struct. Geol.* **2**, 397–410.

Ramsay, J. G. & Huber, M. I. 1987. *Techniques of Modern Structural Geology Volume 2: Folds and Fractures*. Academic Press, London.

Reches, Z. 1978. Analysis of faulting in three-dimensional strain field. *Tectonophysics* **47**, 109–129.

Walsh, J. J. & Watterson, J. 1991. Geometric and kinematic coherence and scale effects in normal fault systems. In: *The Geometry of Normal Faults* (edited by Roberts, A. M., Yielding, G. & Freeman, B.). *Spec. Pub. geol. Soc. Lond.* **56**, 193–203.

Woods, E. P. 1988. Extensional structures of the Jabiru Terrace. In: *The North West Shelf, Australia* (edited by Purcell, P. G. & Purcell, R. R.). *Proc. Explorat. Soc. Australia Symp., Perth*, 1988, 311–330.

Woods, E. P. 1992. Vulcan sub-basin fault styles—implications for

hydrocarbon migration and entrapment. *Australian Petrol. Explor. Ass. J.* **32**, 138–158.

Wormald, G. B. 1988. The Geology of the Challis Oilfield–Timor Sea, Australia. In: *The North West Shelf, Australia* (edited by Purcell, P. G. & Purcell, R. R.). *Proc. Explorat. Soc. Australia Symp., Perth*, 1988, 425–437.

Zhao, G. & Johnson, A. M. 1991. Sequential and incremental formation of conjugate sets of faults. *J. Struct. Geol.* **13**, 887–895.